

Layering defect in p35 deficiency is linked to improper neuronal-glia interaction in radial migration

Amitabh Gupta^{1,5}, Kamon Sanada^{1,5}, David T Miyamoto², Susan Rovelstad³, Bagirathy Nadarajah⁴, Alan L Pearlman³, Jan Brunstrom³ & Li-Huei Tsai¹

Several genes essential for neocortical layering have been identified in recent years, but their precise roles in this process remain to be elucidated. Mice deficient in p35—an activator of cyclin-dependent kinase 5 (Cdk5)—are characterized by a neocortex that has inverted layering. To decipher the physiological mechanisms that underlie this defect, we compared time-lapse recordings between p35^{-/-} and wild-type cortical slices. In the p35^{-/-} neocortex, the classic modes of radial migration—somal translocation and locomotion—were largely replaced by a distinct mode of migration: branched migration. Branched migration is cell-autonomous, associated with impaired neuronal-glia interaction and rare in neurons of *scrambler* mice, which are deficient in Dab1. Hence, our findings suggest that inside-out layering requires distinct functions of Reelin and p35/Cdk5 signaling, with the latter being important for proper glia-guided migration.

The six-layered neocortex is formed by sequential waves of postmitotic neurons that migrate radially from the ventricular zone (VZ) to the pial surface. The first wave establishes a subpial layer termed the preplate zone (PPZ), which the second neuronal wave splits into a superficial marginal zone (MZ) and a deeper subplate (SP), forming a cortical plate (CP) in-between. Thereafter, successive waves of neurons expand the CP by migrating through a cell-sparse intermediate zone (IZ) that separates the SP from the VZ, and they migrate past their neuronal predecessors to arrive directly below the MZ. Hence, neocortical layers are generated in an 'inside-out' manner, with early- and later-migrating neurons forming the deep and superficial CP layers, respectively¹.

Radial migration in the neocortex occurs primarily by two distinct migration modes, locomotion or translocation. Neurons moving by locomotion²⁻⁴ migrate along radial glial fibers²⁻⁶, and their cell body and leading edge move in unison to maintain constant length. Neurons moving by translocation, originally called nuclear translocation⁷⁻¹⁶ but in the neocortex more recently referred to as somal translocation¹⁷, propel their cell somata toward a leading edge that is stably attached to the pial surface and MZ, which effectively shortens neuronal length. Imaging of the embryonic neocortex¹⁷ shows that locomotion and translocation peak at different developmental times: early on, around PPZ-splitting, neurons move radially by translocation, whereas later on, when inside-out layering is underway, they first locomote across the IZ into the CP^{17,18} before translocating to the top CP layer. To date, several signaling pathways have been identified to crucially regulate neocortical layering, including Reelin/VLDLR/ApoER2/Dab1, Cdk5/p35/p39, Lis1, Dlx and filamin-1 (refs. 19–25). Although these pathways affect the early and late phases of neocorti-

cal development distinctly, little is known about how they relate to the different migration modes.

p35 is a regulatory activator of Cdk5. In mice deficient for p35 (refs. 26,27) or Cdk5 (refs. 28–30), the PPZ splits properly, but subsequent waves of migrating neurons fail to move past their predecessors, resulting in a CP with inverted layering. Despite the ample molecular evidence that implicates p35/Cdk5 in regulating neuronal function^{31–35}, it remains unclear how Cdk5 signaling specifically influences the cellular physiology of neuronal migration behavior. To address this issue in the neocortex, we performed comparative time-lapse imaging on acute cortical slices of p35 null and wild-type mice.

Here we report that p35^{-/-} neurons migrate by 'branched migration'. This distinct mode of radial migration, characterized by extensive branching, is cell-autonomous and noticeably associated with altered glial guidance. Considering that wild-type neurons locomote during inside-out layering, these results suggest that proper glia-guided migration is important for this process and requires p35/Cdk5 function. Furthermore, as branched migration was not observed in defective Reelin signaling, which also shows layer inversion, p35/Cdk5 and Reelin signaling seem to contribute distinctly to inside-out layering.

RESULTS

Branched migration occurs early in p35 deficiency

p35^{-/-} neurons presumably migrate normally at embryonic day 13 (E13), when the PPZ splits²⁷. To assess whether this assumption is true, we imaged acute E13 cortical slices of wild-type and p35 null mice. In both genotypes, the dorsal aspect of the anterior neocortex was imaged, as the inverted layering phenotype of the p35^{-/-} neocor-

¹Department of Pathology, Harvard Medical School and Howard Hughes Medical Institute, Boston, Massachusetts 02115, USA. ²Department of Cell Biology, Harvard Medical School, Boston, Massachusetts 02115, USA. ³Departments of Neurology and Cell Biology, Washington University School of Medicine, St. Louis, Missouri 63110, USA. ⁴Division of Neuroscience, School of Biological Sciences, University of Manchester, Manchester M13 9PT, UK. ⁵These authors contributed equally to this work. Correspondence should be addressed to L.H.T. (Li-Huei_Tsai@hms.harvard.edu).

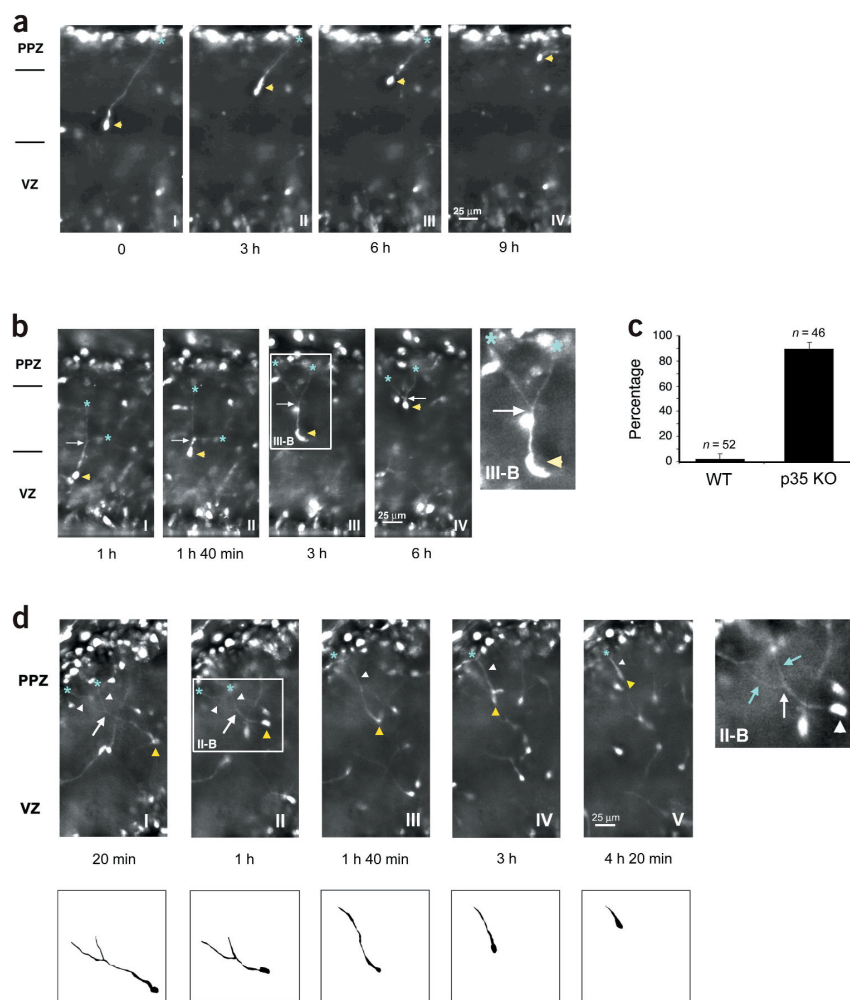


Figure 1 Migration behavior at E13. **(a)** Somal translocation of a wild-type neuron. The leading process (blue asterisk) is attached to the upper preplate zone (PPZ) at all times, allowing the cell soma (yellow arrowhead) to translocate from halfway within the cortex into the PPZ, effectively shortening neuronal length. **(b)** Branched migration of a $p35^{-/-}$ neuron. The leading process is branched, with the leading edges (asterisks) not attached to the PPZ. The cell soma (arrowhead) propels towards the stably positioned branch point (arrow). Significant radial advancement occurs when the cell soma moves through two successive branch points (II–III). Right (III–B), 2 \times magnification shows branching morphology. **(c)** Quantification of the zig-zag trajectory of radially migrating $p35^{-/-}$ neurons. Depicted are percentages of wild-type (WT) and $p35^{-/-}$ neurons that change the direction of migration by an angle larger than 30 $^{\circ}$ per hour. Whereas WT neurons adhere to a strictly radial path, $p35^{-/-}$ neurons change direction during radial migration, reflecting their zig-zag trajectory (n , number of neurons). **(d)** Splitting the $p35^{-/-}$ PPZ involves transition from branched migration to somal translocation. Top, after exiting the VZ by branch migration, with the branches contacting the developing subplate (I,II), the cell soma then enters the PPZ by somal translocation, moving along an unbranched process (III–V) from a previous branch point to the developing marginal zone. Right (II–B), 2 \times magnification shows branching. Yellow arrowhead, cell soma; white arrow, branch point; white arrowhead (I,II) and blue arrow (II–B), branches; arrowhead (III–V), unbranched leading process; asterisk, leading edge. Bottom, tracings emphasize branch points and branches of the leading process.

tex is manifested in a graded manner, decreasing from anterior to posterior and from dorsomedial to ventrolateral²⁶.

Consistent with a previous report¹⁷, we found that 90% of E13 wild-type neurons (27 of 30 neurons selected randomly from six cortical slices) migrated in the radial direction by somal translocation, which occurred in an undisrupted, straight trajectory (Fig. 1a). By contrast, such migration behavior was not seen in the E13 $p35^{-/-}$ neocortex. Rather, $p35^{-/-}$ neurons showed extensive branching morphology (Fig. 1b and Supplementary Fig. 1a online), which was confirmed by silver impregnations of $p35^{-/-}$ cortical sections (data not shown) and green fluorescent protein (GFP) labeling of migrating neurons *in utero* (Supplementary Fig. 1b online and Figs. 3d and 4b). The extensive branching made $p35^{-/-}$ deficient neurons move in a manner that we refer to as branched migration, occurring with a frequency of 83% (25 of 30 radially migrating neurons selected randomly from six cortical slices). Neurons moved by propelling their cell somata along the leading process toward a stably fixed branch point (Fig. 1b and Supplementary Video 1 online).

As the branch points of the migrating $p35^{-/-}$ neurons were found at various locations below the PPZ, radial movement seemed to occur in a disrupted multi-step fashion, distinct from the defined one-step fashion seen in the wild-type neocortex. Indeed, when $p35^{-/-}$ neurons were followed individually over longer periods of time, they traversed much of the neocortex by advancing their cell somata from one branch point to the next (Fig. 1b). Two features of this 'branch-to-

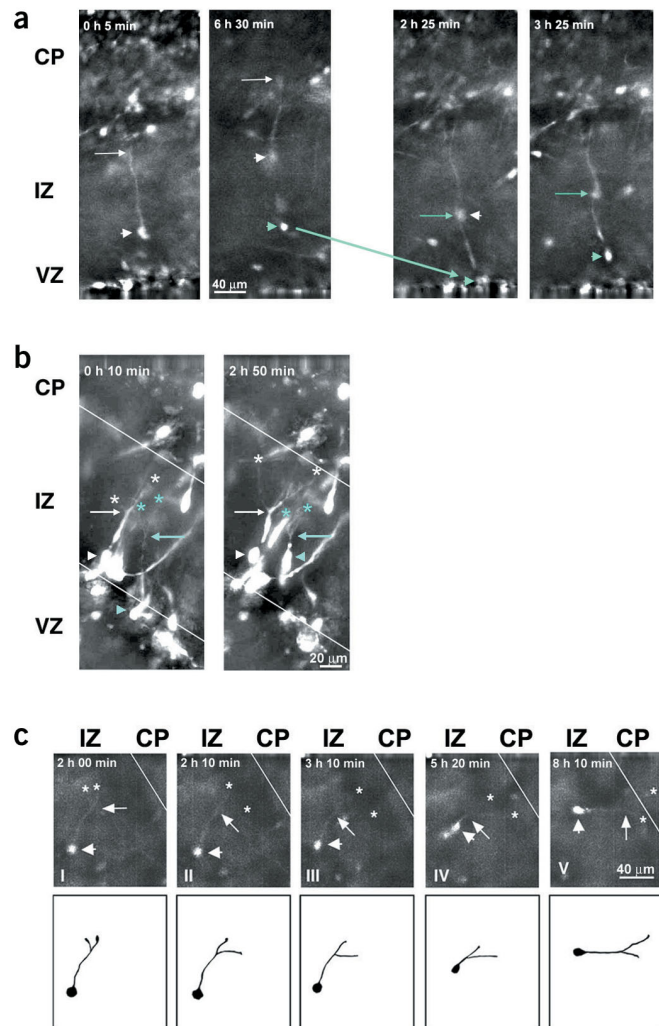
branch' migration were striking. First, branching was very dynamic, indicating that the branches change their length and direction very rapidly, until they are finally locked into position (see Supplementary Fig. 2 online). Second, although branched migration allowed the $p35^{-/-}$ neurons to move in an overall radial direction, the trajectory of the actual movement was more of a 'zig-zag' quality (Fig. 1c and Supplementary Fig. 3 online).

In agreement with proper PPZ splitting, $p35^{-/-}$ deficient neurons were seen to migrate all the way to the developing MZ. However, branched migration was not used for the entire radial journey, but rather until the PPZ was reached. To split the PPZ, $p35^{-/-}$ neurons moved along unbranched processes that were attached to the developing MZ (Fig. 1d), making the final ascent appear indistinguishable from somal translocation (compare Fig. 1a and 1d right). Together, the results indicate that normal layering in the E13 $p35^{-/-}$ neocortex is not associated with a normal pattern of radial migration. Instead, neurons cross most of the neocortex by branched migration before splitting the PPZ by somal translocation.

Branched migration replaces locomotion in $p35$ deficiency

We next conducted our imaging analysis at E15, when inverted layering is evident in the $p35^{-/-}$ neocortex, and migrating neurons actively contribute to the progression of this defect. We reasoned that imaging at E15 should capture defects in migration behavior that are crucial to the phenotype of inverted layering.

Figure 2 Migration behavior at E15. (a) E15 wild-type neurons locomote in tandem. Left, a neuron locomotes radially, maintaining a constant neuronal length, as cell soma (arrowhead) and leading edge (arrow) move coordinately. After some time, a second neuron (green arrowhead) appears, which locomotes along the radial path of the first neuron (right), with its leading edge (green arrow) tucked behind the cell soma of the first one. (b) Branched migration in the E15 $p35^{-/-}$ neocortex. Two neurons (white and blue arrows) migrate by branched migration across the lower IZ, to a location where wild-type neurons would usually locomote. In both cases, cell somata (arrowheads) approach a branch point (arrows) stably positioned far below the CP. The leading edges of the process branches (asterisks) are not attached to the marginal zone. (c) Branch-to-branch migration. Top, time-lapse sequence showing a neuron in the IZ. After dynamic changes of the leading branches (compare position of asterisks in I and II), the cell soma (arrowhead) moves through two consecutive branch points (arrows in II–V), within a change of 35° in the radial trajectory. Bottom, camera lucida-like drawings outline the morphology of the neuronal branches. CP, cortical plate; IZ, intermediate zone; VZ, ventricular zone.



Consistent with previous reports¹⁸ that locomotion accounts for 60–80% of total radial migration at E15, we found that 66% of E15 wild-type neurons used locomotion as their mode of radial migration (20 of 30 radially moving neurons selected at random from ten cortical slices). In the lower part of the neocortex, locomotion was present at 86% (18 of 21 neurons randomly chosen from ten cortical slices), emphasizing that it is the principal mode of radial migration across the IZ at later developmental stages¹⁷ (Fig. 2a and Supplementary Video 2 online). Hence, our imaging procedure recapitulates not only the migration patterns but also the predominance of locomotion previously observed in the E15 wild-type neocortex.

The pattern of radial migration in the $p35$ -deficient neocortex was markedly different. Neurons did not move by locomotion, but by branched migration to effectively traverse the IZ in the radial direction (Fig. 2b and Supplementary Video 3 online). Indeed, branched migration was the principal mode of radial migration at E15, contributing with 93% (24 of 26 cells) to the overall radial migration, with the residual 7% (2 of 26 cells) remaining inconclusive. When followed over longer time periods, individual neurons showed a migration behavior very much like that observed at E13: considerable dynamic branching (Fig. 2c) and ‘branch-to-branch’ migration in a zig-zag pattern (Fig. 2c and Supplementary Fig. 4 online). Furthermore, the branches of the leading processes never reached the pial surface, as branch points were distributed almost exclusively within the IZ (95%), with the remainder positioned in the lower CP (5%).

Branched migration associates with altered glial guidance

Two observations from the imaging study suggest that branched migration might be a glia-independent migration. First, glia-guided locomoting cells always possessed an unbranched leading process (Fig. 2a and Supplementary Video 2 online). Second, unlike the unwavering radial path of locomoting cells (Fig. 2a), branched migration had a zig-zag trajectory (Figs. 1c and 2c and Supplementary Fig. 3 online). For mechanistic evidence of this idea, we made use of the finding that a wild-type radial glia cell (RGC) gives rise to neurons that migrate along their mother glial process³⁶ (Fig. 3a, left). We reasoned that investigating the migration behavior of clonal descendents in the $p35^{-/-}$ neocortex should disclose a possible loss of normal neuronal-glia interaction associated with branched migration. $p35^{-/-}$ neurons could either use one of their branches to move along glia or, alternatively, move independently of glia altogether (Fig. 3b).

As retrovirus selectively targets precursor cells^{36–38}, we labeled individual neuronal clones by introducing a GFP-carrying retrovirus

in utero into E12 $p35^{-/-}$ embryos, and then we assessed the clonal relationship at E15 by GFP-immunostaining. In the posterior neocortex (Fig. 3a, right), which is barely affected by the $p35$ deficiency^{26,27}, the clonal relationship closely resembled that of the wild-type neocortex³⁶. As with locomoting wild-type cells (Fig. 3c, top), clonal descendents of the posterior $p35^{-/-}$ neocortex traversed the IZ in the radial direction along the glial processes of their respective mother cells (RGCs), demonstrating elongated cell somata and unbranched leading processes. Only near the pia did neurons switch to translocation, with their leading processes occasionally arborized to extensively contact the MZ¹⁷ (Fig. 3a, right).

The anterior neocortex, the primary area affected by the $p35$ deficiency, showed an entirely different picture. Migrating $p35^{-/-}$ neurons showed extensive branching across the IZ, and these neurons were not associated with the glial processes of their mother cells (Fig. 3c, bottom). The average distance between their cell bodies and the mother glia was $20.6 \mu\text{m}$ (3.5 cell diameters), with the branches not aligned or attached to the glial process (Fig. 3d). Because we detected branched neurons as early as in the subventricular zone (Fig. 3c), $p35^{-/-}$ neurons appeared to detach very early from their mother cell to migrate as branched cells in the radial direction. In sum, these *in vivo* results suggest that branched neurons have a compromised neuronal-glia interaction, supporting the deductions made from our imaging studies.

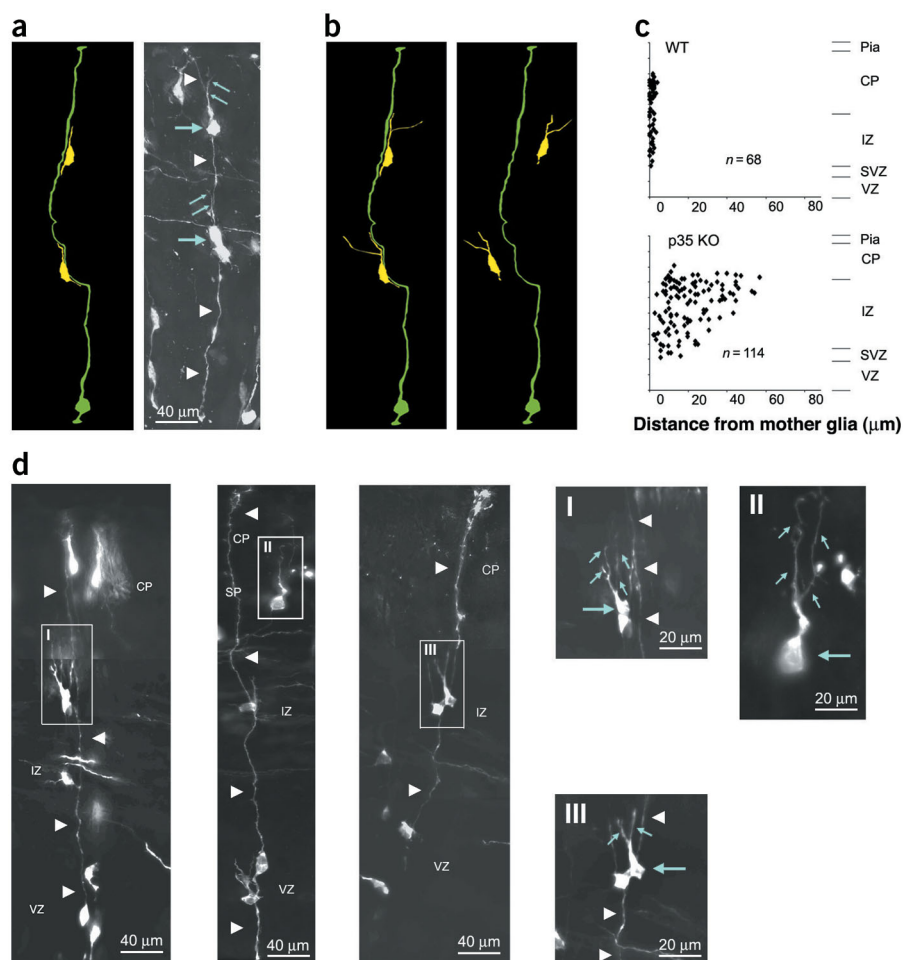


Figure 3 Relationship between migrating neurons and radial glia. (a) Normal migration behavior of clonal descendants. Left, schematic drawing of a wild-type neuronal clone. Right, normal clonal migration behavior in the posterior $p35^{-/-}$ neocortex. Note the switch to glia-independent migration near the pia. (b) Possible relationships between $p35^{-/-}$ neurons and radial glia during branched migration in the radial direction. (c) Branched neurons in the anterior $p35^{-/-}$ neocortex do not associate with their mother glia. The distance of locomoting wild-type (WT) neurons and branched $p35^{-/-}$ neurons from their mother glia is plotted against their distance from the ventricular surface. Whereas WT neurons maintain close contact with their mother glia (top), $p35^{-/-}$ neurons detach early on and stay detached throughout their radial journey (bottom). (d) Representative examples of three migrating neurons in the anterior $p35^{-/-}$ neocortex with branched leading processes (I–III). All three cell bodies are not associated with the mother glia (cell body in III is in a different z-plane than the radial glia, data not shown). Magnifications of I and III emphasize that individual branches are separated from the mother glia fiber. Magnification of II provides a better view of the branching. Large arrow, cell soma; small arrow, leading process branch; arrowhead, radial glia fiber; CP, cortical plate; IZ, intermediate zone; MZ, marginal zone; SP, subplate; VZ, ventricular zone; n = number of cells from eight different embryos.

Branched migration is cell-autonomous in p35 deficiency

To investigate whether branching is cell-autonomous, we electroporated p35 into the $p35$ -deficient neocortex and assessed whether branching could be rescued in those neurons that expressed p35. In electroporation, plasmid DNA is injected *in utero* into the ventricle of embryonic brains and taken up by ventricle-lining cells after exposure to an electrical field³⁹ (Fig. 4a). By using plasmid DNA, we avoided potential toxic effects associated with virus-based methods.

We electroporated $p35^{-/-}$ mice at E13, either with GFP alone or with GFP and p35, and assessed neuronal morphology by GFP-immunostaining at E17. Using an IRES-based plasmid allowed us to detect p35 expression through the GFP label. Just as seen in the imaging experiment, $p35^{-/-}$ neurons showed extensive branching of their leading process when expressing GFP alone (Fig. 4b). Notably, however, when GFP and p35 were applied together, GFP-labeled neurons showed unbranched leading processes (Fig. 4c), which made them look like locomoting wildtype neurons. This rescue occurred independently of where the migrating neuron was positioned along the radial axis of the neocortex (Fig. 4c) and was highly significant (93%; Fig. 4d). Thus, we conclude that branching is a cell-autonomous feature of the migrating neuron.

We further observed that p35-expressing neurons were positionally shifted toward the pial surface in comparison to GFP-expressing neurons alone (Fig. 4e). This shift was most pronounced within the IZ, where the majority of p35-expressing neurons were concentrated in the upper IZ. In contrast, many more $p35$ -deficient neurons were located in the lower IZ. Within the CP, the proportion of neurons was

similar between the two groups, reflecting the fact that early-born neurons successfully split the PPZ and that rescue of cell positioning was partial. Considering that embryos were killed 4 d after electroporation, p35-expressing neurons may have eventually settled within the CP, given sufficient time. Hence, cell positioning in the $p35^{-/-}$ neocortex may also have a cell-autonomous component.

Branched migration is rare in the *scrambler* mouse

Finally, we investigated whether branched migration is restricted to p35 deficiency, given that numerous other mouse mutants harbor distinct neocortical layering defects. We were particularly interested in mice with a defective Reelin signaling pathway^{19–22}, which includes the extracellular matrix protein Reelin, the Reelin receptors ApoER2 and VLDLR, and Dab1, an adaptor protein that binds the Reelin receptors intracellularly^{40–46}. In mice deficient for Reelin, Dab1, or both ApoER2 and VLDLR, neocortical layering is approximately inverted, as it is in the $p35$ deficiency^{23–25}.

To evaluate migration behavior resulting from defective Reelin signaling, we imaged the *scrambler* neocortex, which is Dab1-deficient^{45,46}. We imaged at E15 when, just like in p35 deficiency, layer inversion is very pronounced. In contrast to $p35^{-/-}$ neurons, most Dab1-defective neurons did not show any branching morphology and moved radially by locomotion (Fig. 5a), in a proportion indistinguishable from that observed in the wild-type neocortex of identical strain background (Fig. 5b). To confirm that the locomoting neurons seen in our video analysis were attached to radial glia, we conducted a clonal analysis in the E15 *scrambler* neocortex, using the same condi-

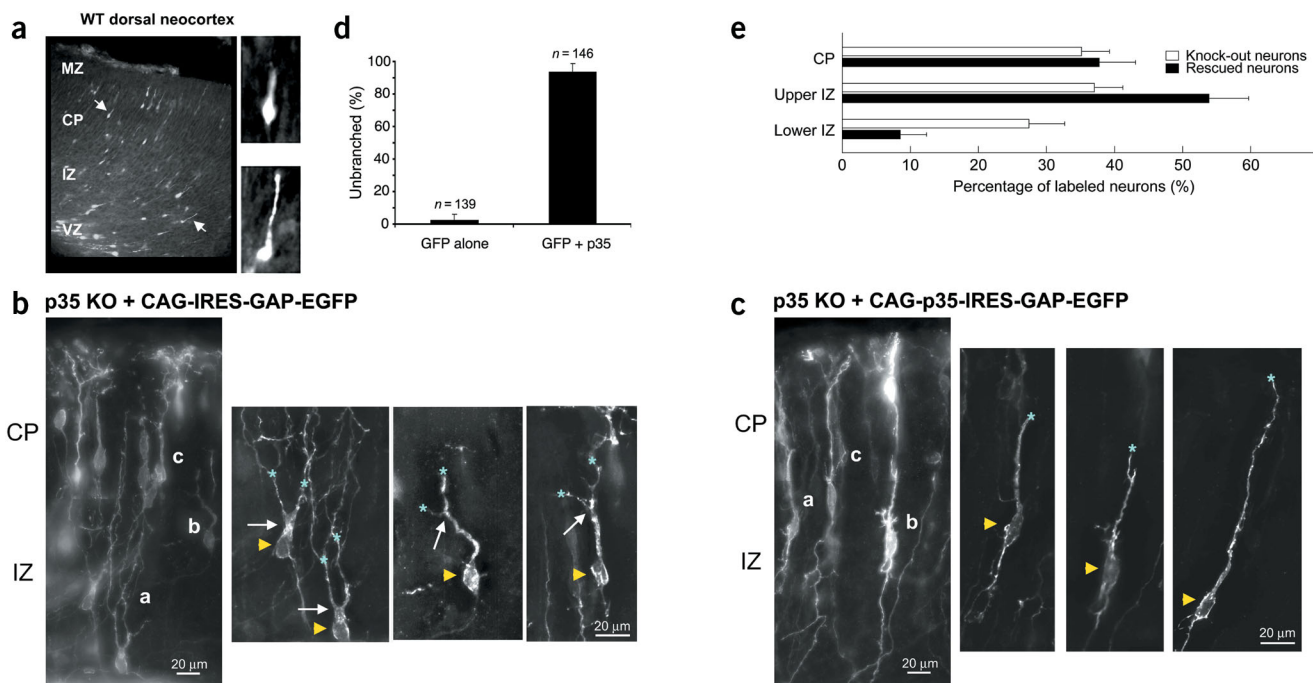


Figure 4 Cell-autonomous functions of p35. **(a)** Electroporation into the anterior dorsal neocortex of a wild-type mouse. Unbranched migrating neurons are seen at various radial positions (arrowheads indicate cells that are magnified). **(b,c)** Branched migration is cell-autonomous. Labeled neurons express **(b)** GFP-alone or **(c)** GFP and p35 in the p35-deficient neocortex. Left, overview of a representative field within the anterior dorsal neocortex. Labeled neurons **(a–c)** are seen in various focal planes with different positions along the radial axis. Right, higher magnifications of individual focal planes. **(d)** Quantification of the rescue of branching. From experiments like in **b** and **c**, the leading process morphology of randomly selected p35^{-/-} neurons was assessed for control (GFP alone) and rescue (GFP + p35) groups. Percentages of unbranched neurons are presented for each group (highly significant difference: $P < 0.0001$; two-tailed, unpaired student *t*-test). **(e)** Radially migrating neurons expressing p35 protein in the anterior p35^{-/-} neocortex move farther toward the cortical plate. The position in relation to the radial axis of the neocortex was assessed for 220 knockout neurons (GFP alone) and 113 rescued neurons (GFP and p35) in six neocortical p35^{-/-} sections. Percentage of labeled neurons is graphed against neocortical regions. Data shown as mean \pm s.e.m. In the wild-type neocortex, 91% of neurons were located in the cortical plate under the same experimental conditions (data not shown). CP, cortical plate; IZ, intermediate zone; arrowhead, cell soma; arrow, branch point; asterisk, leading edge; *n* = number of cells.

tions as in the p35^{-/-} neocortex. Migrating *scrambler* neurons indeed moved along the glial process of their mother cell (Fig. 5c), indicating that branched migration is rarely detected in the *scrambler* mouse at later stages of neocortical development. Therefore, branched migration seems to reflect a defect in p35/Cdk5 but not Reelin signaling.

DISCUSSION

Somal translocation and locomotion peak during PPZ-splitting and inside-out migration, respectively¹⁷. In p35-null mice, PPZ-splitting is preserved, whereas the CP is inverted^{26,27}. This raises the possibility that p35^{-/-} neurons can translocate but not locomote, with the disruption of locomotion contributing to inverted layering. However, we found that in p35 deficiency, both migration modes are affected, as neurons move by branched migration, a distinct migration mode. Here we discuss the precise nature of this defect and the insight it offers into understanding neocortical layering.

Branched migration prevails in the p35^{-/-} neocortex

The alteration of translocation and locomotion in p35 deficiency shows that both modes of radial migration, although distinct in their phenotype and migratory behavior, are not regulated by distinct signaling pathways. Rather, they share common signaling components that may regulate them differentially. Moreover, as branched migration typically accompanied PPZ-splitting in p35^{-/-} mice, abnormal migration behavior does not necessarily affect neocortical structure.

At E15, however, the abundance of branched migration (Fig. 2b,c) does suggest that altered migration behavior may relate to inverted layering in p35 deficiency. As branched migration replaces locomotion at that time, compromised locomotion is tied to defective inside-out layering, with branched migration inadequately compensating for this compromise.

Branch-to-branch migration (Figs. 1b and 2c) seems to be a mechanism for maximizing the advancement of p35^{-/-} neurons in the radial direction. The dynamic nature of branching (Fig. 2c and **Supplementary Video 3** online) supports this idea, suggesting that migrating neurons explore their environment to proceed as far as possible. Without branch-to-branch migration, the lower part of the p35^{-/-} neocortex might be filled with permanently and randomly arrested neurons that fail to split the PPZ or form a layered CP. However, advancement by this migration may also come at a cost, as its zig-zag trajectory may contribute to the delayed net movement seen in p35 deficiency^{26,27}.

At E15, we also observed branched migration in radially migrating wild-type neurons, but only in 7% of cases. This concurs with recent evidence that links wild-type branched migration to radially migrating interneurons⁴⁷, which are known to migrate independently of Cdk5 activity³⁰. We confirmed by calbindin staining that branched neurons in the p35 null mice are principally not interneurons (data not shown). If branched migration of p35^{-/-} projection neurons is analogous to that of wild-type interneurons, projection neurons may

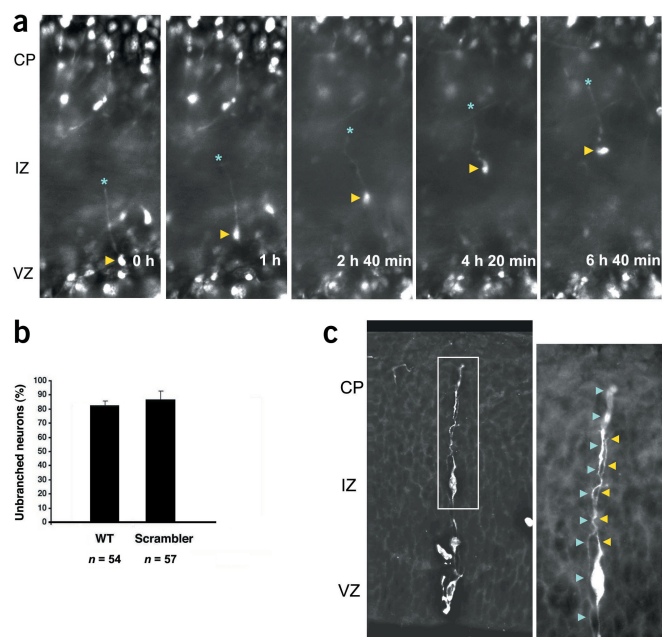


Figure 5 Migration behavior of *scrambler* neurons. **(a)** Branched migration is not evident in the E15 *scrambler* neocortex. The representative neuron crosses the intermediate zone (IZ) by locomotion: unlike $p35^{-/-}$ neurons, *scrambler* neurons have unbranched leading processes. Arrowhead, cell soma; asterisk, leading edge. **(b)** *Scrambler* and wild-type (WT) neocortices show similar proportions of unbranched migrating neurons at E15. Migrating WT and *scrambler* neurons were randomly selected from anterior neocortical sections 2 d after infection with a GFP-carrying retrovirus. For each category, three different embryos were assessed and results plotted as percentage of unbranched neurons (n = number of cells). **(c)** *Scrambler* neurons use glial guides in the E15 neocortex. The representative neuron shown (box) is attached with its cell soma and unbranched leading process (yellow arrowheads) to the glial process of its mother cell (blue arrowheads).

possess the basic machinery for radial migration, but may require p35/Cdk5 to translocate or locomote at the appropriate developmental stage. p35/Cdk5 may actively suppress branching, indicating that establishing an unbranched process for translocation or locomotion may have an inhibitory component.

Branched migration, abnormal glial guidance and cell autonomy

Our *in vivo* data showing that branched neurons do not use their mother glia (Fig. 3) offers a cellular mechanism for inverted layering in p35 deficiency: the failure to use glial guides may account for the inability to migrate past neuronal predecessors. Although branched neurons could use non-mother glial guides, this possibility seems less likely. First, wild-type neurons principally use their mother glia to migrate in the radial direction³⁶ (our retroviral studies). Second, in the absence of any known functional or structural differences between neighboring glia, branched neurons are unlikely to selectively use non-mother glial guides, when unable to move along mother glia. Hence, our clonal analysis suggests that inside-out layering may depend on proper neuronal-glia interaction, proposing an explanation for why the loss of glia-guided locomotion cannot be entirely compensated for by branched migration and why locomotion emerges with inside-out migration in normal development. In support of this idea, positionally shifted neurons in our rescue experiment (Fig. 4e) resembled locomoting neurons.

Cell-autonomy of branching (Fig. 4c,d) indicates that branching results from a p35 deficiency in migrating neurons and not from compromised neuronal-neuronal or neuronal-glia interactions requiring Cdk5 activity in surrounding neurons. Further, it shows that branching is caused by a p35 deficiency that manifests itself at the point of development studied and not by a secondary effect arising from a p35 deficiency exerted earlier in development. The fact that the rescue effect was not absolute suggests that some p35-electroporated neurons were radially migrating interneurons or were not expressing p35 protein at the appropriate level and time.

Distinct Cdk5 and Reelin signaling in inside-out layering

As E15 *scrambler* neurons, unlike $p35^{-/-}$ neurons, move by locomotion (Fig. 5), glia-guided migration is necessary but not sufficient

for inside-out layering. The mechanisms of inverted layering are different in the p35/Cdk5 and Dab1 deficiencies, suggesting that p35/Cdk5 and Reelin functions are arranged in parallel, rather than serial, signaling pathways to regulate distinct aspects of inside-out layering. Migrating neurons deficient in Reelin signaling appear to be unable to detach from radial glia⁴⁸. Curiously, this stands at the opposite spectrum of our result in p35 deficiency, but at the same time has in common with it a principal compromise in proper neuronal-glia interaction. Our cellular results fit well with the increasing molecular evidence that supports a parallel relationship between p35/Cdk5 and Reelin signaling^{49,50}.

Reconciling migration behavior and structural development

Why is branched migration compatible with PPZ-splitting, but not inside-out migration? PPZ-splitting requires a proper response of migrating neurons to Reelin, which is secreted from the developing MZ to presumably act locally^{20,21,23}. It seems plausible that $p35^{-/-}$ neurons retain proper responsiveness to Reelin, after reaching its vicinity by branched migration. This notion fits with a parallel arrangement of the Cdk5 and Reelin signaling pathways^{49,50} (Fig. 5) and with our result that $p35^{-/-}$ neurons enter the PPZ by somal translocation (Fig. 1e). Hence, PPZ-splitting may occur regardless of how neurons reach Reelin, as long as they respond to it, with somal translocation being part of this response.

Conversely, inside-out migration appears to be incompatible with branched migration. When the neocortex greatly expands and glia-guided migration prevails, compromised guidance along the mother glia may prevent migration past neuronal predecessors, terminating radial migration at significant distance from Reelin protein. Substrates for branched migration may reside on predecessor neurons or on axonal fiber tracts that aberrantly extend through the p35/Cdk5-compromised neocortex^{27,29}, with sequential attachment to them perhaps promoting branch-to-branch migration. However, the inability to reach Reelin eventually prevents proper positioning underneath the MZ.

METHODS

Imaging of acute brain slices. p35 null mice were compared to wild-type mice of equivalent strain background²⁶. Studies were done in accordance with the guidelines of the Animal Studies Committee at Harvard Medical School and the National Institutes of Health. Acute brain slices were prepared as described previously¹⁷. To visualize neuronal migration, slices were incubated for 2 h in DMEM/F12 media, containing 10 μ g/ml Oregon Green BAPTA-1 488 AM (Molecular Probes) and 0.003% pluronic acid (Molecular Probes) transferred onto poly-D-lysine- and collagen-coated glass coverslips (22 mm²; Corning) and overlaid with additional collagen (Vitrogen from Cohesion) for immobilization. After incubation for 1 h without medium in a humidified chamber (5% CO₂, 37 °C) and then for 2 h in DMEM/F12 medium with 1 \times N₂-

Supplement (Gibco), coverslips were fitted into a temperature-controlled (37 °C) chamber clamped onto the microscope stage. Slices were maintained by continuous perfusion (40 ml/h) with oxygenated DMEM/F12 medium (pH 7.4), enriched with 1× N₂-Supplement and 20 mM Hepes.

Labeled cells were viewed through a 20× water-immersion objective (NA 0.75) of a Nikon inverted microscope (488 nm excitation and 522/535 nm emission filters). Images were collected with a cooled CH-350 CCD camera (Roper Scientific) every 10 min as image stacks of 4–6 z-steps (5 μm), with the most superficial image being 40 μm below the slice cut surface. After individual z-sections were deconvoluted (Delta Vision software from Applied Precision), z-sections of each time point were projected onto each other and fused to a movie (NIH Image software).

Clonal analysis. Pregnant p35 null or *scrambler* mice were anesthetized with avertin at E12, their uterine horns exposed, and 2 μl of virus solution injected into the lateral ventricle of each embryo with a glass micropipette. After development for 3 more days *in utero*, embryonic brains were dissected and subjected to GFP immunostaining.

A replication-incompetent retrovirus was used for the *in utero* injection, which expresses enhanced GFP (EGFP) from the vector pMX-GFP (gift from T. Kitamura, University of Tokyo). Retrovirus was concentrated by centrifugation at 100,000g for 3 h, and precipitated virus particles were diluted in OPTI-MEM at a concentration of 1 × 10⁸ c.f.u./ml. Prior to injection, virus solution was complemented with 200 mg/ml polybrene and 0.01% Fast Green solution.

p35 rescue experiment. p35 was electroporated into the developing embryo as described previously³⁹. The plasmid backbone used was pCAGGIG (gift from T. Matsuda, Harvard Medical School). This EGFP expression vector is driven by the CAG promoter and directs EGFP expression through the internal ribosomal entry site (IRES). To obtain distal expression, GFP was targeted to the membrane by adding to its N terminus the amino acid sequence MLCCMRRTKQVEEKNDDEDQKI of the GAP-43 protein. We then used this modified CAG-IRES-GAP-EGFP construct to express GFP alone, and the CAG-p35-IRES-GAP-EGFP construct to express GFP together with p35. Plasmid DNA was injected at a concentration of 5 μg/μl in phosphate-buffered saline (PBS).

Tissue preparation and GFP immunohistochemistry. Dissected brains were fixed overnight at 4 °C in 4% paraformaldehyde in PBS, equilibrated for 12–16 h at 4 °C in 30% sucrose in PBS, embedded in O.C.T compound (Sakura Finetek USA Inc.) and frozen in liquid nitrogen. Brains were then cut coronally into 40-μm thick sections with a Leica CM3050 cryostat (Leica Microsystems) and mounted onto Superfrost glass slides (Fisher Scientific).

For GFP immunohistochemistry, cortical sections were blocked for 45 min with 10% goat serum in PBS containing 0.1% Triton X-100 (Sigma) and incubated overnight at 4 °C with a polyclonal anti-GFP antibody (Molecular Probes) diluted at 1:2,000 in blocking solution. The secondary antibody used was a FITC anti-rabbit antibody (ICN/Cappel) incubated for 2 h at room temperature at 1:400 in blocking solution. Fluorescent images were obtained with a CH-350 CCD camera (Roper Scientific) followed by image deconvolution (Delta Vision).

Note: Supplementary information is available on the Nature Neuroscience website.

ACKNOWLEDGMENTS

The authors thank S. Tobet at the Shriver Center for technical help with the slice procedure, F. Gertler at Massachusetts Institute of Technology, where the quantitative and trajectory analysis was performed with DIAS software, and H. Patzke, M.D. Nguyen, J. Ko and B. Samuels for comments on the manuscript. K.S. is supported by a fellowship from the Naito Foundation. This work was supported by National Institutes of Health grants to L.-H.T. and by research grants from the National Eye Institute (EY00621 to A.L.P.). L.-H.T. is an associate investigator of the Howard Hughes Medical Institute.

COMPETING INTERESTS STATEMENT

The authors declare that they have no competing financial interests.

Received 9 August; accepted 15 October 2003

Published online at <http://www.nature.com/natureneuroscience/>

- Angevine, J.Jr. & Sidman, R.L. Autoradiographic study of cell migration during histogenesis of cerebral cortex in the mouse. *Nature* **192**, 766–768 (1961).
- Rakic, P. Neuron-glia relationship during granule cell migration in developing cerebellar cortex. A Golgi and electron microscopic study in Macacus Rhesus. *J. Comp. Neurol.* **141**, 283–312 (1971a).
- Rakic, P. Guidance of neurons migrating to the fetal monkey neocortex. *Brain Res.* **33**, 471–476 (1971b).
- Rakic, P. Mode of cell migration to the superficial layers of fetal monkey neocortex. *J. Comp. Neurol.* **145**, 61–83 (1972).
- O'Rourke, N.A., Dailey, M.E., Smith, S.J. & McConnell, S.K. Diverse migratory pathways in the developing cerebral cortex. *Science* **258**, 299–302 (1992).
- Edmondson, J.C. & Hatten, M.E. Glial-guided granule neuron migration *in vitro*: a high resolution time-lapse video microscopic study. *J. Neurosci.* **7**, 1928–1934 (1987).
- Pearlman, A.L., Faust, P.L., Hatten, M.E. & Brunstrom, J.E. New directions for neuronal migration. *Curr. Opin. Neurobiol.* **8**, 45–54 (1998).
- Morest, D.K. A study of neurogenesis in the forebrain of opossum pouch young. *Z. Anat. Entwicklungsgesch.* **130**, 265–305 (1970).
- Book, K.J. & Morest, D.K. Migration of neuroblasts by perikaryal translocation: role of cellular elongation and axonal outgrowth in the acoustic nuclei of the chick embryo medulla. *J. Comp. Neurol.* **297**, 55–76 (1990).
- Book, K.J., Howard, R. & Morest, D.K. Direct observation *in vitro* of how neuroblasts migrate: medulla and cochleovestibular ganglion of the chick embryo. *Exp. Neurol.* **111**, 228–243 (1991).
- Hendriks, R., Morest, D.K. & Kaczmarek, L.K. Role in neuronal cell migration for high-threshold potassium currents in the chicken hindbrain. *J. Neurosci. Res.* **58**, 805–814 (1999).
- Hager, G., Dodt, H.-U., Sieglansberger, W. & Liesi, P. Novel forms of neuronal migration in the rat cerebellum. *J. Neurosci. Res.* **40**, 207–219 (1995).
- Yee, K.T., Simon, H.H., Tessier-Lavigne, M. & O'Leary, D.M. Extension of long leading processes and neuronal migration in the mammalian brain directed by the chemoattractant netrin-1. *Neuron* **24**, 607–622 (1999).
- Gray, G.E. & Sanes, J.R. Migratory paths and phenotypic choices of clonally related cells in the avian optic tectum. *Neuron* **6**, 211–225 (1991).
- Snow, R.L. & Robson, J.A. Migration and differentiation of neurons in the retina and optic tectum of the chick. *Exp. Neurol.* **134**, 13–24 (1995).
- Brittis, P.A., Meiri, K., Dent, E. & Silver, J. The earliest pattern of neuronal differentiation and migration in the mammalian central nervous system. *Exp. Neurol.* **133**, 1–12 (1995).
- Nadarajah, B., Brunstrom, J.E., Grutzendler, J., Wong, R.O.L. & Pearlman, A.L. Two modes of radial migration in early development of the cerebral cortex. *Nat. Neurosci.* **4**, 143–150 (2001).
- Miyata, T., Kawaguchi, A., Okano, H. & Ogawa, M. Asymmetric inheritance of radial glial fibers by cortical neurons. *Neuron* **31**, 727–741 (2001).
- Cooper, J.A. & Howell, B.W. Lipoprotein receptors: signaling functions in the brain? *Cell* **97**, 671–674 (1999).
- Bar, I., Lambert de Rouvroit, C. & Goffinet, A.M. The evolution of cortical development. An hypothesis based on the role of the Reelin signaling pathway. *Trends Neurosci.* **23**, 633–638 (2000).
- Rice, D.S. & Curran, T. Role of the reelin signaling pathway in central nervous system development. *Annu. Rev. Neurosci.* **24**, 1005–1039 (2001).
- Herz, J. The LDL receptor gene family: (un)expected signal transducers in the brain. *Neuron* **29**, 571–581 (2001).
- Gilmore, E.C. & Herrup, K. Cortical development: receiving reelin. *Curr. Biol.* **10**, R162–166 (2000).
- Gupta, A., Tsai, L.H. & Wynshaw-Boris, A. Life is a journey: a genetic look at neocortical development. *Nat. Rev. Genet.* **3**, 342–355 (2002).
- Feng, Y. & Walsh, C. Protein-protein interactions, cytoskeletal regulation and neuronal migration. *Nat. Rev. Neurosci.* **2**, 408–416 (2001).
- Chae, T. *et al.* Mice lacking p35, a neuronal specific activator of Cdk5, display cortical lamination defects, seizures, and adult lethality. *Neuron* **18**, 29–42 (1997).
- Kwon, Y.T. & Tsai, L.H. A novel disruption of cortical development in p35(–/–) mice distinct from reeler. *J. Comp. Neurol.* **395**, 510–522 (1998).
- Ohshima, T. *et al.* Targeted disruption of the cyclin-dependent kinase 5 gene results in abnormal corticogenesis, neuronal pathology and perinatal death. *Proc. Natl. Acad. Sci. USA* **93**, 11173–11178 (1996).
- Gilmore, E.C., Ohshima, T., Goffinet, A.M., Kulkarni, A.B. & Herrup, K. Cyclin-dependent kinase 5-deficient mice demonstrate novel developmental arrest in cerebral cortex. *J. Neurosci.* **18**, 6370–6377 (1998).
- Gilmore, E.C. & Herrup, K. Neocortical cell migration: GABAergic neurons and cells in layers I and VI move in a cyclin-dependent kinase 5-independent manner. *J. Neurosci.* **21**, 9690–9700 (2001).
- Nikolic, M., Dudek, H., Kwon, Y.T., Ramos, Y.F. & Tsai, L.H. The cdk5/p35 kinase is essential for neurite outgrowth during neuronal differentiation. *Genes Dev.* **10**, 816–825 (1996).
- Nikolic, M., Chou, M.M., Lu, W., Mayer, B.J. & Tsai, L.H. The p35/Cdk5 kinase is a neuron-specific Rac effector that inhibits Pak1 activity. *Nature* **395**, 194–198 (1998).
- Kwon, Y.T., Gupta, A., Zhou, Y., Nikolic, M. & Tsai, L.H. Regulation of N-cadherin-mediated adhesion by the p35-Cdk5 kinase. *Curr. Biol.* **10**, 363–372 (2000).
- Niethammer, M. *et al.* NUDEL is a novel Cdk5 substrate that associates with LIS1 and cytoplasmic dynein. *Neuron* **28**, 697–711 (2000).
- Sasaki, S. *et al.* A LIS1/NUDEL/cytoplasmic dynein heavy chain complex in the developing and adult central nervous system. *Neuron* **28**, 681–696 (2000).

36. Noctor, S.C., Flint, A.C., Weissman, T.A., Dammerman, R.S. & Kriegstein A.R. Neurons derived from radial glial cells establish radial units in neocortex. *Nature* **409**, 714–720 (2001).
37. Walsh, C. & Cepko, C.L. Clonally related cortical cells show several migration patterns. *Science* **241**, 1342–1345 (1988).
38. Luskin, M.B., Pearlman, A.L. & Sanes, J.R. Cell lineage in the cerebral cortex of the mouse studied *in vivo* and *in vitro* with a recombinant retrovirus. *Neuron* **1**, 635 (1988).
39. Tabata, H. & Nakajima, K. Efficient in utero gene transfer system to the developing mouse brain using electroporation: visualization of neuronal migration in the developing cortex. *Neuroscience* **103**, 865–872 (2001).
40. D'Arcangelo, G. *et al.* A protein related to extracellular matrix proteins deleted in the mouse mutant reeler. *Nature* **374**, 719–723 (1995).
41. D'Arcangelo, G. *et al.* Reelin is a ligand for lipoprotein receptors. *Neuron* **24**, 471–479 (1999).
42. Hiesberger, T. *et al.* Direct binding of Reelin to VLDL receptor and ApoE receptor 2 induces tyrosine phosphorylation of disabled-1 and modulates tau phosphorylation. *Neuron* **24**, 481–489 (1999).
43. Howell, B.W., Hawkes, R., Soriano, P. & Cooper, J.A. Neuronal position in the developing brain is regulated by mouse disabled-1. *Nature* **389**, 733–737 (1997).
44. Trommsdorff, M. *et al.* Reeler/Disabled-like disruption of neuronal migration in knockout mice lacking the VLDL receptor and ApoE receptor 2. *Cell* **97**, 689–701 (1999).
45. Sheldon, M. *et al.* Scrambler and yotari disrupt the disabled gene and produce a reeler-like phenotype in mice. *Nature* **389**, 730–733 (1997).
46. Ware, M.L. *et al.* Aberrant splicing of a mouse disabled homolog, mdab1, in the scrambler mouse. *Neuron* **19**, 239–249 (1997).
47. Nadarajah, B., Alifragis, P., Wong, R.O. & Parnavelas, J.G. Ventricle-directed migration in the developing cerebral cortex. *Nat. Neurosci.* **5**, 218–224 (2002).
48. Pinto-Lord, M.C., Evrard, P. & Caviness, V.S.Jr. Obstructed neuronal migration along radial glial fibers in the neocortex of the reeler mouse: a Golgi-EM analysis. *Brain Res.* **256**, 379–393 (1982).
49. Keshvara, L., Magdaleno, S., Benhayon, D. & Curran, T. Cyclin-dependent kinase 5 phosphorylates disabled 1 independently of Reelin signaling. *J. Neurosci.* **22**, 4869–4877 (2002).
50. Beffert, U. *et al.* Reelin-mediated signaling locally regulates PKB/Akt and GSK-3 β . *J. Biol. Chem.* **277**, 49958–49964 (2002).